# Coherent Bremsstrahlung in the $\alpha + p$ System at 50 MeV/nucleon

M. Hoefman,[1] L. Aphecetche,[2,*] J. C. S. Bacelar,[1] H. Delagrange,[2,*] P. Descouvemont,[3] J. Díaz,[4] D. d'Enterria,[2,*] M.-J. van Goethem,[1] R. Holzmann,[5] H. Huisman,[1] N. Kalantar-Nayestanaki,[1] A. Kugler,[6] H. Löhner,[1] F. M. Marqués,[7] G. Martínez,[2,*] J. G. Messchendorp,[1] R. W. Ostendorf,[1] S. Schadmand,[1,†] R. H. Siemssen,[1,‡] R. S. Simon,[5] Y. Schutz,[2,*] R. Timmermans,[1] R. Turrisi,[1,§] M. Volkerts,[1] V. Wagner,[6] H. Weller,[8] H. W. Wilschut,[1] and E. Wulf[8]

[1]*Kernfysisch Versneller Instituut, Zernikelaan 25, NL-9747 AA Groningen, The Netherlands*
[2]*Grand Accélérateur National d'Ions Lourds, F-14076 Caen Cedex 5, France*
[3]*Université Libre Bruxelles CP229, B-1050 Brussels, Belgium*
[4]*Instituto de Física Corpuscular, E-46100 Burjassot, Spain*
[5]*Gesellschaft für Schwerionenforschung, D-64291 Darmstadt, Germany*
[6]*Nuclear Physics Institute, 25068 Řež u Prahy, Czech Republic*
[7]*Laboratoire de Physique Corpusculaire, F-14050 Caen Cedex, France*
[8]*TUNL Duke University, Durham, North Carolina 27708-0308*

(Received 28 March 2000)

Photons originating from coherent bremsstrahlung have been measured over a large dynamic range for the reaction of 200 MeV $\alpha$ particles with protons. At low photon energies the bremsstrahlung spectrum exhibits the classical behavior with an approximate $1/E_\gamma$ shape. At higher photon energies there is a pronounced contribution from capture into the unbound ground state and first excited state of $^5$Li. These results allow one, for the first time, to test theoretical models for a consistent description of bremsstrahlung and radiative capture in a complex system. Calculations predict both features qualitatively but fail to account for their relative importance.

PACS numbers: 25.10.+s, 25.40.Lw, 25.40.Cm, 25.40.Ep

With the recent focus on hard photons produced in intermediate energy and relativistic nucleus-nucleus collisions [1] the interest in the underlying basic processes of bremsstrahlung production has been renewed. In earlier research a range of mechanisms including coherent and incoherent processes was considered [2]. It is now generally assumed that incoherent bremsstrahlung production from the individual nucleon-nucleon collisions in a reaction is the dominating process [3]. The search for coherent bremsstrahlung has since been abandoned, and the question whether, or under what conditions, coherent bremsstrahlung can still contribute remained unanswered.

To investigate this aspect we have searched for coherent bremsstrahlung in the $\alpha + p$ system at 50 MeV/nucleon. Because of the strong binding of the $\alpha$ particle, the quasifree process can lead only to bremsstrahlung with $E_\gamma < 22$ MeV, while at higher energy, up to the kinematic limit of $E_{\max} = 39$ MeV, bremsstrahlung can only be produced coherently in this reaction. In fact, we find coherently produced hard photons to be the dominant radiative process in the $\alpha + p$ system. By measuring scattered particles in coincidence with photons, the complete kinematics can be recovered and the coherent bremsstrahlung spectrum can be extended to photon energies below 22 MeV, where incoherent processes may contribute. The difference with the inclusive spectrum implies a rapid onset of incoherent bremsstrahlung. The coherent bremsstrahlung spectrum appears to exhibit two components, classical bremsstrahlung with a $1/E_\gamma$ dependence and radiative capture into the unbound system $^5$Li. The dynamic range of the present bremsstrahlung data allows one to test for the first time the consistency of models that attempt to describe these two aspects within a single theoretical framework.

This study was part of the experimental program with the photon spectrometer TAPS [4–6] at the AGOR facility of the Kernfysisch Versneller Instituut. A beam of 200 MeV $\alpha$ particles with a typical intensity of 0.4 pnA was incident on a liquid hydrogen target [7] contained in a 6 mm thick aluminum frame with thin (0.55 mg/cm$^2$) window foils. After filling, the amount of hydrogen corresponded to a nominal thickness of 56 mg/cm$^2$. The contribution of the windows to the photon spectrum was measured with an empty target frame and was corrected for. External conversion of photons was minimized and kept below 1% by the use of a 70 cm diameter carbon-fiber scattering chamber with a wall thickness of 4 mm.

The photon spectrometer TAPS was configured in six blocks of 64 $BaF_2$ crystals, each at a distance of 66 cm from the target. The setup covered the polar angular range between 57° and 176° on both sides of the beam, with a vertical acceptance of 42°. The granularity of the TAPS setup resulted in an angular resolution better than 5°. Photons were separated from nuclear particles via their time of flight with respect to the radio frequency (rf) signal of the cyclotron. The time resolution of about 2 ns (FWHM) was mainly determined by the cyclotron system. In addition, pulse-shape discrimination was employed. The event trigger required an energy deposition of at least 5 MeV in a $BaF_2$ module. The signals from the plastic veto detectors in front of the $BaF_2$ scintillators were used to

 0031-9007/00/85(7)/1404(4)$15.00 

suppress charged particles. Photons in the energy range between 10 and 40 MeV are measured with an energy resolution better than 8%. The relative energy calibration was determined from the characteristic energy deposited by cosmic-ray muons. The absolute calibration was provided by the 15.1 MeV photons originating from excited $^{12}$C nuclei populated by reactions in the target windows. This state also provided an accurate method to subtract the background from the target window by requiring that the 15.1 MeV contribution be completely eliminated. A small residual background from cosmic-ray muons within the trigger gate was removed by subtracting a photon spectrum obtained by gating on a random time window with respect to the rf. The charged particles were measured in a forward cone between 6° and 19° with the small-angle large-acceptance detector (SALAD) [8]. SALAD consists of two multiwire proportional counters followed by plastic scintillators. The reaction channel associated with coherent bremsstrahlung could be determined from the energies and angles of the detected particles.

After transformation to the $\alpha + p$ center of mass (c.m.) frame, the spectra at all angles exhibit the same characteristic shape as shown in Fig. 1. The shape of this spectrum is very different from that of the hard photons in nucleus-nucleus reactions, for which exponential slopes are observed. The pronounced peak just below the kinematical limit is characteristic for radiative capture. The data in Fig. 1 have been obtained by integrating over the TAPS acceptance and extrapolating to $4\pi$ solid angle as shown in Fig. 2, where the photon angular distribution in the c.m. system is shown for $E_\gamma > 22$ MeV. The data were obtained for a narrow band of 8° in azimuthal angle to avoid acceptance fluctuations. A third order Legendre polynomial fit to the measured angular distribution allowed one to extrapolate to the full solid angle with a systematic uncertainty of 3%. The absolute cross section was deduced from the known target thickness and the integrated beam current, corrected for dead time. The systematic error due to the uncertainty of the beam intensity and the target thickness is 5%.

Exclusive photon spectra were obtained by detecting the photons in coincidence with either the $\alpha$ particle or the proton, or both. The kinematics is overdetermined only in the latter case. The resulting spectrum is shown in Fig. 3. The solid circles result from events with overdetermined kinematics (triple coincidences) in a restricted dynamic range, while the open circles result from events with determined kinematics (double coincidences). The latter data cover the full dynamic range but may contain a small contribution from incorrectly interpreted events below $E_\gamma = 22$ MeV. The absolute cross section was obtained by matching the exclusive spectra to the inclusive spectra in the coherent regime above 22 MeV. For $E_\gamma < 20$ MeV the cross section does not increase with decreasing photon energy as fast as the inclusive cross section (Fig. 1). This is because below $E_\gamma = 22$ MeV the incoherent processes start to contribute rapidly as the phase space for such processes increases. Small differences between the spectra in Figs. 1 and 3 for $E_\gamma > 20$ MeV reflect the differences and uncertainties in the acceptance for the inclusive and exclusive data. The acceptance has been calculated on the basis of the potential model, but is determined nearly model independent due to the large probability of 40%–60% that photons detected in TAPS are accompanied by a particle in SALAD [9].

In the following, we interpret the exclusive data in terms of classical bremsstrahlung on the one hand and radiative capture on the other. A classical bremsstrahlung spectrum

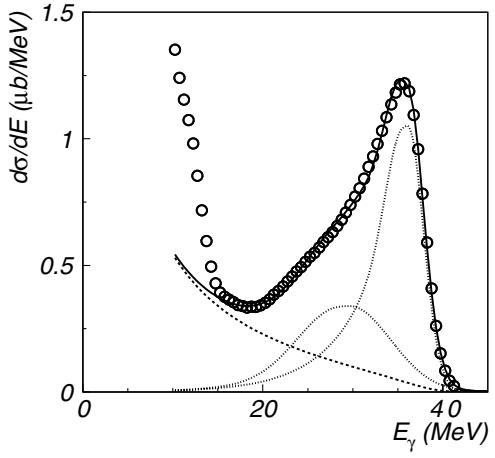


FIG. 1. Inclusive photon-energy spectrum (in the c.m. frame) for the $\alpha + p$ reaction at 50 MeV/nucleon. The statistical errors are smaller than the symbols. The global fit (solid line) is decomposed into the classical bremsstrahlung spectrum (dashed line) and two contributions representing capture to the two low-lying resonances in $^5$Li, i.e., the unbound ground state and the first-excited state (dotted lines).

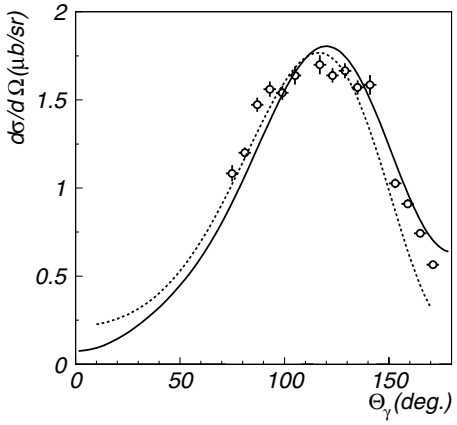


FIG. 2. Inclusive photon angular distribution in the c.m. frame for $E_\gamma > 22$ MeV. The vertical error bars are statistical only; the horizontal bars indicate the bin width. Two predictions are indicated: the potential model (×1.6) of [12] (solid line) and the shape of a classical electrodynamics calculation [9,21] (dashed line, arbitrarily normalized).

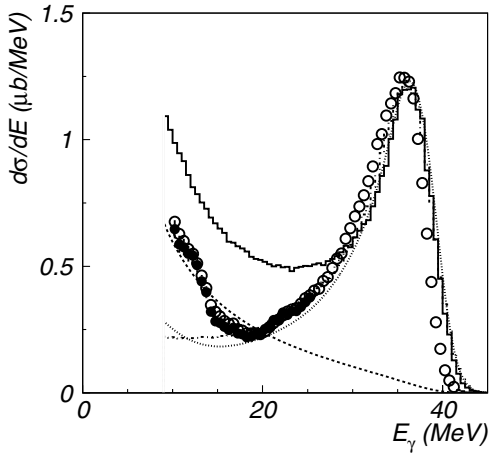


FIG. 3. Coherent bremsstrahlung spectrum (in the c.m. frame) obtained from kinematically complete events by requiring double (○) and triple (●) coincidences; see text. The dashed line represents the classical bremsstrahlung spectrum identical to that shown in Fig. 1. The solid and dashed-dotted histograms are obtained from calculations with the potential model (×1.6) and the soft-photon approximation (×1.26), respectively. The dotted line represents a standard radiative-capture calculation (×0.75).

obeying energy and momentum conservation depends on the photon energy, $E_\gamma$, as [10]

$$\frac{d\sigma}{dE_\gamma} \propto \frac{1}{E_\gamma}\sqrt{1 - E_\gamma/E_{\max}}\,, \qquad (1)$$

where $E_{\max} = 39$ MeV is the maximum possible photon energy. In Fig. 3 we find such a dependence to follow the shape of the bremsstrahlung spectrum between 10 and 20 MeV. The remaining part can be qualitatively understood in terms of radiative capture populating the unbound ground and first excited state of $^5$Li.

We have fitted the photon energy spectrum by assuming that it consists of two Gaussian peaks and a background according to Eq. (1), folded with the asymmetric energy response of the TAPS detectors according to Ref. [5]. We neglect a possible mixing phase between the various components. The free parameters in the fit are the individual FWHM widths ($\Gamma$), the cross sections ($\sigma$) for the two states, and their positions in energy ($E_x$); see Table I. The fit was restricted to $E_\gamma > 22$ MeV and the result is shown in Fig. 1 (solid line) together with the two individual components (dotted lines). The widths of the two peaks and their positions are consistent with the adopted values for the two lowest resonances of $^5$Li [11]. The cross section for $10 < E_\gamma < 22$ MeV (in the c.m. frame) associated with the coherent nonresonant component is $\sigma = 4.8 \pm 1.0$ $\mu$b, and that associated with photons from incoherent processes is $\sigma = 2.3 \pm 1.0$ $\mu$b. The latter is obtained from the difference of the inclusive and the exclusive data. The errors are systematic and associated with residual uncertainties in the acceptance.

TABLE I. Parameters of the $^5$Li resonances deduced from the exclusive photon-energy spectrum and previous values obtained with conventional $R$-matrix theory.

| $J^\pi$ | | Present data | $R$ matrix [11] |
|---|---|---|---|
| $\frac{3}{2}^-$ | $\sigma$ ($\mu$b) | 8.0 ± 0.7 | – |
| | $E_x$ (MeV) | 2.9 ± 0.2 | 2.08 |
| | $\Gamma$ (MeV) | 1 ± 0.2 | 2.11 |
| $\frac{1}{2}^-$ | $\sigma$ ($\mu$b) | 4.5 ± 0.4 | – |
| | $E_x$ (MeV) | 9.3 ± 0.4 | 8.26 |
| | $\Gamma$ (MeV) | 10 ± 1 | 19.8 |

Clearly, the decomposition of the angle-integrated spectrum into a classical bremsstrahlung and a radiative capture component qualitatively describes the data. However, in a consistent bremsstrahlung model both aspects should be described simultaneously. To this end we have compared the present data with three different models.

The potential model of Baye *et al.* [12] accurately treats the computational problems associated with transitions to continuum states and with the Coulomb contribution. In the present calculations the so-called Kanada potential [13] was employed that reproduces the elastic scattering phase shifts of the $\alpha + p$ system. The restriction to real potentials is not considered to be a severe limitation for the $\alpha + p$ system because of the high breakup threshold of the $\alpha$ particle. In Fig. 3 the potential-model calculation (solid histogram), folded with the detector response, is compared with the exclusive spectrum. The model cross sections were multiplied with a factor 1.6 to match the peak cross section of the data. The model describes the rapid decrease as a function of energy and the enhancement in the capture region. However, this calculation would fit the low-energy region without the normalization factor. Hence the model can not quantitatively account for the classical and the capture component of the bremsstrahlung spectrum simultaneously.

Various implementations of the soft-photon approximation can be found in the literature. It has been applied with some success to the $\alpha + p$ bremsstrahlung in previous studies at proton energies between 7 and 45 MeV. However, the data of these experiments were very limited [14]. To describe processes with resonances in the final state, a covariant generalization of the Feshbach-Yennie approximation [15,16] was applied to the present data. The input is the experimentally known elastic-scattering phase shifts [17]. The result of this calculation, multiplied by a normalization factor of 1.26, is compared (dashed-dotted histogram) with the data in Fig. 3 after folding with the TAPS response. This calculation, however, underestimates the data at the lower energies. Its classical $(1/E_\gamma)$ behavior sets in at a much lower photon energy (a few MeV, not shown in the figure).

An additional calculation, which extends the model of direct capture into bound states to the case of direct capture into unbound states, was performed using the technique of Ref. [18] and is shown as the dotted line in Fig. 3. This

calculation employed a complex optical model potential, obtained from fitting the elastic-scattering angular distributions [19], to describe the incoming channel. The energy dependent real potential [20], used to describe the two lowest states of $^5$Li, was constructed to reproduce the experimentally determined elastic-scattering phase shifts. The normalization factor in this case is 0.75. This model follows the soft-photon approximation quite well in shape, although the classical region appears to set in at higher energy, but still underestimates by far the data.

The shape of the angular distribution is quite well predicted by all models. As an example we show in Fig. 2 the potential-model prediction (solid line). In fact, a calculation based on classical electrodynamics [9,21] already reproduces the shape (dashed line), indicating that it is determined by the charge asymmetry of the system as a consequence of direct capture.

In the capture part of the cross section we find agreement between all three models within a factor of 2. The variations at low photon energies are much larger. The opening of inelastic reaction channels in this energy region, e.g., the resonances decaying into $d + {}^3$He, may require a more detailed description than available from any of the models. A coupled-channel approach may be necessary. Note that the models differ strongly in the treatment of the absorption. For a proper understanding of nuclear bremsstrahlung it is desirable to learn for which photon and beam energies coherent bremsstrahlung approaches the classical dependence, and to establish the role of the nuclear structure of projectile and target. Experimentally, one can study these aspects for the present system by measuring the photon spectra as a function of beam energy. In particular, at higher energy the dynamic range below the breakup threshold could be extended, and its possible impact on the coherent bremsstrahlung mechanism could be studied more extensively.

In summary, we have observed hard photons associated with coherent bremsstrahlung in the $\alpha + p$ reaction. Photon-particle coincidences allowed us to extend the coherent bremsstrahlung spectrum to photon energies as low as 10 MeV. The low-energy photon spectrum appears to have a classical $1/E_\gamma$ shape. Photons with energies close to the kinematic limit have been associated with direct capture to the two lowest states of the unbound $^5$Li. The data have been compared with model calculations in which coherent bremsstrahlung and direct capture are treated consistently as the same process. The calculations qualitatively reproduce these two features of the data but do not reproduce their relative magnitude.

The tireless effort of the AGOR crew in providing the beam is greatly appreciated. This work is part of the research program of the "Stichting voor Fundamenteel Onderzoek der Materie" (FOM) with financial support from the "Nederlandse Organisatie voor Wetenschappelijk Onderzoek" (NWO), The Netherlands, the IN2P3 and CEA, France, by the BMBF and DFG, Germany, by the DGICYT and the Generalitat de València, Spain, by the GACR, Czech Republic, and by the European Union HCM Network under Contract No. HRXCT94066.

*Present address: Laboratoire SUBATECH, BP 20722, F-44307 Nantes Cedex 3, France.
†Present address: II. Physikalisches Institut, Universität Gießen, D-35392 Gießen, Germany.
‡Present address: Argonne National Laboratory, Argonne, Illinois 60439.
§Present address: Dipartimento di Fisica Galileo Galilei, I-35131 Padova, Italy.

[1] Y. Schutz *et al.,* Nucl. Phys. **A622**, 404 (1997), and references therein.
[2] H. Nifenecker and J. P. Bondorf, Nucl. Phys. **A442**, 478 (1985).
[3] H. Nifenecker and J. A. Pinston, Annu. Rev. Nucl. Part. Sci. **40**, 113 (1990).
[4] H. Ströher, Nucl. Phys. News **6**, 7 (1996).
[5] A. R. Gabler *et al.,* Nucl. Instrum. Methods Phys. Res., Sect. A **346**, 168 (1994).
[6] F. M. Marqués *et al.,* Nucl. Instrum. Methods Phys. Res., Sect. A **365**, 392 (1995).
[7] N. Kalantar-Nayestanaki, J. Mulder, and J. Zijlstra, Nucl. Instrum. Methods Phys. Res., Sect. A **417**, 215 (1998).
[8] N. Kalantar-Nayestanaki *et al.,* Nucl. Instrum. Methods Phys. Res., Sect. A **444**, 591 (2000).
[9] M. Hoefman, Ph.D. thesis, Rijksuniversiteit Groningen, 1999.
[10] J. Ashkin and R. E. Marshak, Phys. Rev. **76**, 58 (1949).
[11] F. Ajzenberg-Selove, Nucl. Phys. **A490**, 1 (1988); D. R. Tilley *et al.,* Nucl. Phys. (to be published). The resonance parameters depend strongly on the choice of $R$-matrix theory.
[12] D. Baye *et al.,* Nucl. Phys. **A550**, 250 (1992).
[13] H. Kanada *et al.,* Prog. Theor. Phys. **61**, 1327 (1979).
[14] W. Wölfli, J. Hall, and R. Müller, Phys. Rev. Lett. **27**, 271 (1971); A. M. Green and A. Prodon, Nucl. Phys. **A183**, 225 (1972); G. A. Anzalon *et al.,* Nucl. Phys. **A255**, 250 (1975).
[15] Z. M. Ding, D. Lin, and M. K. Liou, Phys. Rev. C **40**, 1291 (1989).
[16] M. K. Liou, R. G. E. Timmermans, and B. F. Gibson, Phys. Lett. B **345**, 372 (1995).
[17] D. C. Dodder *et al.,* Phys. Rev. C **15**, 518 (1977); A. Houdayer *et al.,* Phys. Rev. C **18**, 1985 (1978); G. M. Hale (private communication).
[18] H. R. Weller *et al.,* Phys. Rev. C **25**, 2921 (1982).
[19] C. M. Perey and F. G. Perey, At. Data Nucl. Data Tables **17**, 1 (1976).
[20] G. R. Satchler *et al.,* Nucl. Phys. **A112**, 1 (1968).
[21] M. Hoefman *et al.,* Nucl. Phys. **A654**, 779c (1999).